The Electronic Structures of Linear Dicyano Complexes

Mitsuru SANO,* Hirohiko ADACHI,† and Hideo YAMATERA††

Laboratory of Inorganic Chemistry, Faculty of General Education, Nagoya University, Nagoya 464
†*Department of Nuclear Engineering, Faculty of Enginneering, Osaka University, Suita 565*
††*Department of Chemistry, Faculty of Science, Nagoya University, Nagoya 464*

(Received June 11, 1981)

Molecular orbital (MO) calculations in the discrete variational Xα (DV-Xα) scheme have been made on linear dicyano complexes, $[Ag(CN)_2]^-$, $[Au(CN)_2]^-$, and $[Hg(CN)_2]$, to clarify their electronic structures. The valence X-ray photoelectron spectra (XPS) for these compounds are also reported. The calculated energy levels are consistent with the XPS results. The relative magnitudes of the bond overlap populations show a good correlation with those of the force constants obtained from infrared data. The calculated MO features show that the mixing of the metal $(n+1)$s orbital is important in stabilizing the linear L–M–L bonds, especially in the partial cancellation of the antibonding character of the σ_g-type highest occupied molecular orbital.

Cyanide complexes have various symmetrical structures belonging to the $D_{\infty h}$, T_d, D_{4h}, and O_h point groups; the simplest of these is a linear two-coordinate complex, NC–M–CN ($D_{\infty h}$), which is formed by heavier ions with d^{10} configuration, such as Ag^+, Au^+, and Hg^{2+}. The study of the linear coordinate bond, L–M–L, is very important for inorganic chemists because it is one of the fundamental structures of coordination compounds. Orgel[1] has attributed the tendency of the d^{10} ions to form linear complexes to the d—s mixing rather than to the special stability of s—p hybrid bonds. Thus, the d_z^2 and s orbitals can be mixed together to give two new orbitals: $(1/\sqrt{2})(d_{z^2}-s)$ and $(1/\sqrt{2})(d_{z^2}+s)$. If the $(1/\sqrt{2})(d_{z^2}-s)$ orbital were occupied and the $(1/\sqrt{2})(d_{z^2}+s)$ orbital left empty, then the ligands in the x-plane would be repelled and a complex ion extending along the z-axis would be stable. However, Orgel's theory does not explain how the metal-ligand bond is formed. Moreover, Mason[2] has carried out absorption and magnetic-circular-dichroism spectral measurements for some linear dicyano complexes and has rejected the argument that metal d orbital predominantly participate in the metal-ligand σ bonding.

We have previously studied the electronic structures of octahedral[3–5] and square-planar[6] cyanide complexes. The studies on the electronic structures of the linear dicyano complexes of Ag^+, Au^+, and Hg^{2+} will complete a series of studies on cyanide complexes. In order to discuss the electronic structures of linear two-coordinate complexes, a systematic investigation of a few representative complexes has been made by means of the molecular orbital (MO) calculations and the measurements of valence X-ray photoelectron spectra (XPS).

Experimental

The complexes studied here are all well-known and were prepared by standard methods. The valence-region X-ray photoelectron spectra were recorded on a JEOL Model JESCA-3A spectrometer. Magnesium $K\alpha_{1,2}$ radiation (1253.6 eV) was used as the X-ray excitation source and the measurements were carried out at a vacuum of 5×10^{-7} Torr (7×10^{-5} Pa) or below.

Computational Method

The computations have been carried out by the discrete-variational Xα (DV-Xα) method, the details of which have been described elsewhere.[7] In the Hartree-Fock-Slater model,[8] the exchange-correlation term is give by

$$V_{xc}(1) = -3\alpha[(3/8\pi)\rho(1)]^{1/3}$$

where $\rho(1)$ is the local charge density and α is the exchange scaling parameter; the value, $\alpha=0.70$, is used for all atoms throughout the present calculations.[9] The DV-Xα self-consistent-charge (SCC) procedure[10] has been performed, where an approximate self-consistent molecular potential is determined from the Mulliken gross orbital populations. The numerical basis functions are obtained with an atom-like potential constructed by spherically averaging the molecular potential around the nucleus for the region inside each atomic sphere.[10] The basis sets include Ag 1s—5p, Au and Hg 1s—6p, and C and N 1s—2p. The molecular geometries for the complexes are assumed as follows:

Ag–C = 2.02 and C–N = 1.13 Å for $[Ag(CN)_2]^-$,

Au–C = 2.12 and C–N = 1.17 Å for $[Au(CN)_2]^-$,

Hg–C = 2.01 and C–N = 1.14 Å for $[Hg(CN)_2]$.

In the present calculations, the complexes are regarded as having the $D_{\infty h}$ symmetry.

Results and Discussion

The MO's of Free CN^-. The electronic structure of the free cyanide ion is briefly described for convenience of comparison with coordinated cyanide ions. Table 1 shows the orbital energies (with reference to arbitrary zero level) and the Mulliken populations for the free CN^- ion. The contours of the CN^- valence MO's are also shown in Fig. 1. The main features of the CN^- MO's are: (1) the order of the valence MO energies is $3\sigma \ll 4\sigma < 1\pi < 5\sigma$, and (2) the 4σ MO has a higher density on nitrogen, 5σ on carbon, and 1π on nitrogen. The 5σ MO will play the most important role in the coordination of the cyanide ion to a metal ion, and the 4σ, 1π, and 2π MO's also take part in the metal-ligand bond through orbital mixing.

The present result from the DV-Xα calculation and

Table 1. Electronic structure of CN^-

Orbital	Energy/eV	Charge distribution/% C 1s	C 2s	C 2p	N 1s	N 2s	N 2P
2π	11.4			59			41
5σ	3.7		21	41		5	33
1π	2.6			41			59
4σ	0.6		34	8		24	34
3σ	−10.4		22	11		57	10
2σ	−255.8	100					
1σ	−366.6				100		

Carbon orbital	Population	Nitrogen orbital	Population
1s	2.00	1s	2.00
2s	1.54	2s	1.73
$2p\sigma$	1.20	$2p\sigma$	1.54
$2p\pi$	1.63	$2p\pi$	2.37
Atomic charge	−0.37	Atomic charge	−0.63

C–N	Overlap population
2π	−0.598
5σ	−0.194
1π	0.268
4σ	0.002
3σ	0.387

the previous one from an ab initio MO calculation nearly agree in the wavefunction maps,[4] but disagree significantly in the Mulliken populations.[3] The populations are to some extent an artifact and depend on the basis set used in the calculation.[11] The present result showing a higher population on N (in contrast to the previous one showing a higher population on C) is reasonable, considering the electronegativity of N is greater than that of C.

The Natures of MO's. Figure 2 schematically shows the symmetry-allowed interaction between the $(CN^-)_2$ and metal orbitals in a linear cyanide complex. In the formation of the complex, the σ-type metal s (σ_g), $p\sigma$ (σ_u), and $d\sigma$ (σ_g) orbitals interact with the CN^- 4σ and 5σ orbitals, and the π-type metal $d\pi$ (π_g) and $p\pi$ (π_u) orbitals with the CN^- 1π and 2π orbitals. The metal $d\delta$ orbitals do not interact with ligand orbitals because there is no cyanide valence orbital of δ_g symmetry. Table 2 gives the energies and symmetries of the occupied valence MO's together with their atomic components for $[Ag(CN)_2]^-$, $[Au(CN)_2]^-$, and $[Hg(CN)_2]$. Schematical illustrations of the MO energy levels are given in Fig. 3, which also shows the approximate levels of the metal and ligand orbitals for ready comparison. The metal d orbital level is drawn at the same energy as that of the δ_g MO, which consists almost exclusively of the metal $d\delta$ orbital. The level of the CN^- 1π orbital is drawn at the same energy as that of the $6\pi_u$ MO which consists predominantly of the 1π orbital of CN^-; the contributions of the CN^- 2π and the metal $p\pi$ orbitals to this MO are unimportant, as suggested by the orbital populations. Although such layouts of

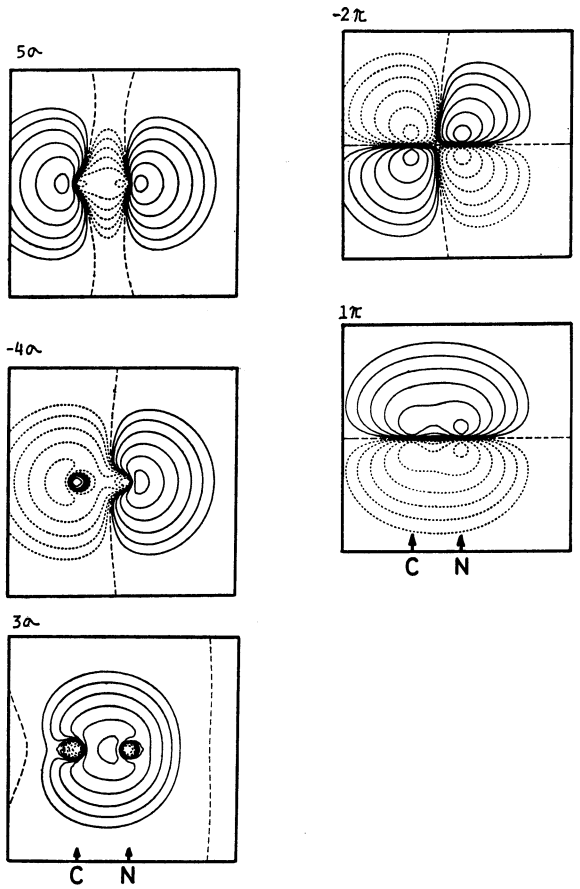

Fig. 1. The wavefunction controus for valence shell MO's of the free CN^- ion. The broken line shows 0.00, and the first solid and dotted contours show ± 0.01, respectively, and neighboring contours differ by a factor of two.

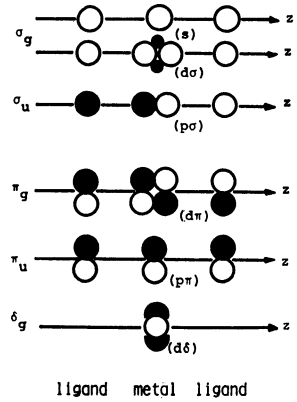

Fig. 2. $D_{\infty h}$ adapted combinations of ligand and metal orbitals.

orbital levels are arbitrary, they show approximate relative positions of the metal and ligand orbital levels in the complexes.

In the case of $[Ag(CN)_2]^-$, selected MO contours are shown in Fig. 4. In the π_g symmetry, the metal $d\pi$ orbital interacts with the 1π and 2π orbitals of CN^-, which lie above the Ag $4d\pi$ orbital. According to the orbital mixing rule,[12] the $2\pi_g$ MO with lower energy

TABLE 2. THE VALENCE SHELL MO's OF $[Ag(CN)_2]^-$, $[Au(CN)_2]^-$, AND $[Hg(CN)_2]$

Symmetry	Energy/eV	Orbital population/%						
		Ag			C		N	
		4d	5s	5p	2s	2p	2s	2p
$11\sigma_g$	−0.77	36.8	28.4		6.7	12.1	2.9	13.1
$3\pi_g$	−0.96	9.1				9.5		61.4
$8\sigma_u$	−1.71			1.3	6.3	21.9	19.2	51.2
$4\pi_u$	−2.52			0.9		48.3		50.7
$10\sigma_g$	−2.70	18.5	1.9		3.2	0.0	28.2	48.2
$2\delta_g$	−3.49	100.0						
$2\pi_g$	−4.00	86.5				12.1		1.3
$7\sigma_u$	−4.63			6.2	42.1	24.1	16.0	11.5
$9\sigma_g$	−6.99	35.7	4.6		27.3	27.6	4.3	0.5
$6\sigma_u$	−16.34			1.5	19.3	15.4	50.2	13.6
$8\sigma_g$	−16.35	0.2	0.7		21.3	13.8	50.4	13.6
		Au			C		N	
		5d	6s	6p	2s	2p	2s	2p
$13\sigma_g$	0.01	46.9	34.4		5.9	7.4	0.4	5.1
$4\pi_g$	−1.34	54.3				10.0		35.7
$10\sigma_u$	−1.74			2.8	9.9	28.7	13.2	45.3
$3\delta_g$	−1.92	100.0						
$6\pi_u$	−2.44			0.9		45.3		53.9
$12\sigma_g$	−2.79	13.8	0.0		0.6	5.6	25.7	54.4
$3\pi_g$	−3.14	41.9				34.0		24.1
$9\sigma_u$	−4.75			5.7	39.5	16.0	20.6	18.1
$11\sigma_g$	−6.47	27.3	6.5		31.2	24.3	8.0	2.7
$10\sigma_g$	−16.07	0.3	0.6		22.0	12.7	52.3	12.0
$8\sigma_u$	−16.07			1.2	20.4	14.2	52.2	12.0
		Hg			C		N	
		5d	6s	6p	2s	2p	2s	2p
$10\sigma_u$	−8.34			1.1	2.31	4.9	24.5	57.1
$13\sigma_g$	−8.38	4.9	14.4		0.9	11.2	20.4	48.1
$4\pi_g$	−8.71	3.7				42.1		54.2
$6\pi_u$	−9.06			1.5		49.5		48.9
$12\sigma_g$	−10.31	27.1	21.8		18.4	5.6	14.2	13.0
$9\sigma_u$	−11.80			8.9	44.3	29.9	11.8	5.0
$3\delta_g$	−13.76	100.0						
$3\pi_g$	−14.14	94.8				4.9		0.4
$11\sigma_g$	−16.31	61.2	2.3		14.3	20.2	2.1	0.0
$10\sigma_g$	−23.08	0.5	0.8		22.3	12.8	49.7	15.9
$8\sigma_u$	−23.09			1.5	19.8	15.0	49.7	14.0

has the dominant contribution from the metal $d\pi$ orbital and consists of the $d\pi+1\pi+2\pi$ combination. (A wavefunction with+sign has positive values in the region between the metal and carbon atoms.) On the other hand, the $3\pi_g$ MO with higher energy is the $1\pi-d\pi-2\pi$ MO (the −sign indicating negative values between M and C), in which the largest component is the 1π orbital. A slight mixing of the 2π orbital with the 1π orbital causes a decrease of the orbital population on nitrogen in the $2\pi_g$ MO and an increase of the same in the $3\pi_g$ MO.

Among σ-type MO's, $6\sigma_u$ and $8\sigma_g$ (not given in Fig. 4) are mainly constructed of the CN^- 3σ orbital. The $7\sigma_u$ and $8\sigma_u$ MO's consist of the $4\sigma+5\sigma+p\sigma$ and $5\sigma-4\sigma-p\sigma$ combinations; the $p\sigma$ orbital of Ag lies far above the 4σ and 5σ orbitals of CN^- and contributes to the MO's only slightly. The calculated orbital populations of these MO's can be explained by assuming an appropriate orbital mixing of the 4σ and 5σ orbitals; thus a mixing of 9: 1 (in the measure of electron-density) gives an estimate of orbital populations (in %) of 49(C2s), 22(C2p), 16(N2s), and 13(N2p) for the $4\sigma+5\sigma$ orbital and 6, 27, 14, and 53 for the $5\sigma-4\sigma$ orbital. These values are very similar to the populations of the $7\sigma_u$ and $8\sigma_u$ orbitals (Table 2). The metal $d\sigma$ ($4d_{z^2}$) and s (5s) orbitals as well as the ligand 4σ and 5σ orbitals belong to the same symmetry, and their energy levels are in the order of $4\sigma<d\sigma<5\sigma<s$. They are mixed together to form the $9\sigma_g$, $10\sigma_g$, and $11\sigma_g$ MO's. The 4σ orbital of CN^- is dominant in the $9\sigma_g$ MO, having

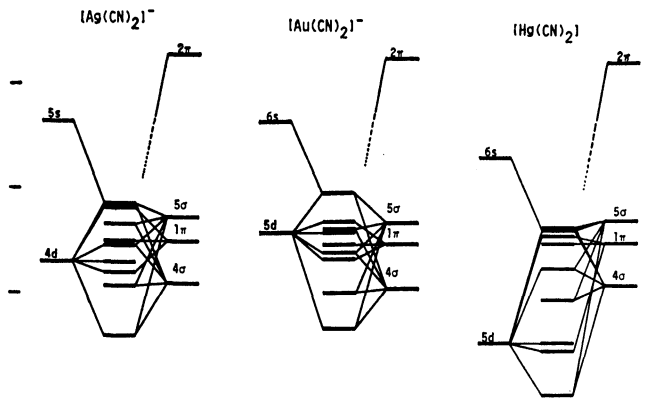

Fig. 3. Schematically illustrated MO energy levels with the levels of metal and cyanide orbitals. The MO level orderings (from the top to the bottom) are: $11\sigma_g$, $3\pi_g$, $8\sigma_u$, $4\pi_u$, $10\sigma_g$, $2\delta_g$, $2\pi_g$, $7\sigma_u$, and $9\sigma_g$ for $[Ag(CN)_2]^-$; $13\sigma_g$, $4\pi_g$, $10\sigma_u$, $3\delta_g$, $6\pi_u$, $12\sigma_g$, $3\pi_g$, $9\sigma_u$, and $11\sigma_g$ for $[Au(CN)_2]^-$; $10\sigma_u$, $13\sigma_g$, $4\pi_g$, $6\pi_u$, $12\sigma_g$, $9\sigma_u$, $3\delta_g$, $3\pi_g$, and $11\sigma_g$ for $[Hg(CN)_2]$.

bonding interactions with the metal orbitals ($4\sigma+5\sigma+d\sigma+s$). Both Table 2 and Fig. 4 show a considerable mixing of the 5σ into the 4σ orbitals (about 4 : 6 in the $9\sigma_g$ MO). They also show that the $10\sigma_g$ MO is nearly nonbonding with regard to the M–C bond and has the highest electron density in the N lone-pair regions; the $10\sigma_g$ wavefunction is expressed as $5\sigma-4\sigma+d\sigma-s$. This minus combination of the 4σ with 5σ orbitals decreases the carbon charge and increases the charge on nitrogen. The HOMO, $11\sigma_g$, is antibonding with respect to the M–C bond and corresponds to a $d\sigma-s$ hybrid orbital with $d\sigma-s-5\sigma(+4\sigma)$ combination (Fig. 5); the antibonding interactions of the $d\sigma$ with the 5σ orbital is relaxed by the mixing of the s orbital of the metal.

In $[Au(CN)_2]^-$, the valence shell MO's are similar to those of the Ag^+ complex. The HOMO is $13\sigma_g$, which corresponds to the $11\sigma_g$ MO of the latter. However, the Au^+ complex gives a slightly different MO level diagram from that for the Ag^+ complex; the relative position of the δ_g MO is higher for the Au^+ complex, indicating that the d level of Au^+ in the complex is higher than that of Ag^+ (Fig. 3). Thus the highest occupied π_g-type orbital, $4\pi_g$, has more the character of the metal $d\pi$ orbital rather than that of the ligand π orbital, while the corresponding orbital of $[Ag(CN)_2]^-$, $3\pi_g$, is characterized as a predominantly ligand orbital.

The atomic d orbital of Hg^{2+} is situated at a lowet energy than those of Ag^+ and Au^+. Thus, in $[Hg(CN)_2]$, the $11\sigma_g$, $3\pi_g$, and $3\delta_g$ MO's are composed predominantly of metal d orbitals, while the HOMO ($10\sigma_u$) is localized mainly on ligands. This feature is very different from those for the Ag^+ and Au^+ complexes. In the σ_g system, the sequence of the orbital energy is $d\sigma<4\sigma<5\sigma<s$. The $11\sigma_g$ MO has the metal $d\sigma$ (d_{z^2}) orbital as the main component, with small contributions of the 4σ, 5σ, and metal s orbitals. This ($d\sigma+4\sigma+5\sigma+s$)-type MO is bonding with respect to the Hg–CN bond. In the $12\sigma_g$ MO, the main component is the 4σ orbital with the combination of $4\sigma-5\sigma-d\sigma+s$, while the 5σ orbital is dominant in the $13\sigma_g$ MO with $5\sigma-4\sigma-d\sigma+s$. The contribution of the metal s orbital in these MO's relaxes the antibonding interaction of the $d\sigma$ with the 4σ or 5σ orbitals, thus strengthening the metal-cyanide bonds.

Main Features of Bonding Structure in NC–M–CN. As can be seen from the MO contours (Fig. 4) and energy-level diagrams (Fig. 3), the σ bond is very strong. This is also suggested by the M–C bond overlap population given in Table 4. The greatest contribution to the stabilization of the complexes is made by the bonding interaction of the metal $d\sigma$ orbital and the ($4\sigma+5\sigma$)-type

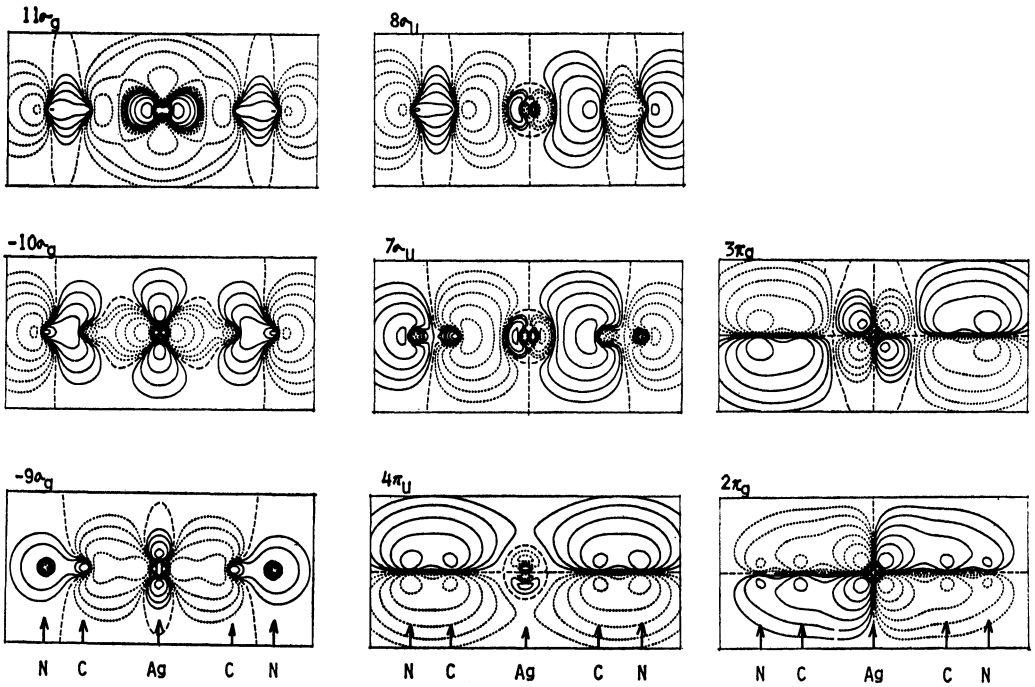

Fig. 4. Selected valence-shell MO contours for $[Ag(CN)_2]^-$.

ligand orbital, resulting in the $9\sigma_g$ (Ag complex) or $11\sigma_g$ (Au and Hg complexes) MO, in which the (dσ+s)-type mixing of the $(n+1)$s with the ndσ orbital also occurs to add a minor contribution to the stabilization of the M–C bond. On the other hand, the (dσ—s)-type metal orbitals interact with the $(5\sigma-4\sigma)$-type ligand orbital to form an antibonding $11\sigma_g$ (Ag complex) or $13\sigma_g$ (Au and Hg complexes) MO, in which the $(n+1)$s orbital is considerably mixed with the ndσ orbital to reduce the antibonding character of the MO. The orbital interactions discussed above are schematically illustrated in Fig. 5.

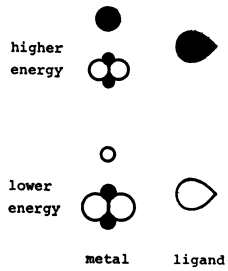

Fig. 5. Orbital interactions of metal dσ and s orbitals and ligand orbitals of σ_g symmetry. (Only one of the ligand orbitals is shown.) The size indicate the magnitudes of orbital components. The positive and negative signs of the orbitals are shown by the white and black area.

The situation mentioned above is in contrast to Orgel's simplified theory,[1] according to which the dσ—s orbital is stabilized while the destabilized dσ+s orbital is empty. However, the bonding structure observed here might be peculiar to the cyanide complexes. In these complexes, the soft cyanide ions strongly interact with the soft noble-metal ion to form bonds of highly covalent character; the cyanide 4σ and 5σ orbitals are mixed with each other to result in the $(4\sigma+5\sigma)$-type orbital, which has an increased electron density at the carbon atoms, and efficiently interact with the metal dσ orbital to form coordinate bonds. Moreover, the small separation of the nd and $(n+1)$s orbital energies (6.7 eV for Ag, 5.7 eV for Au, and 8.8 eV for Hg) results in a large contribution of the metal $(n+1)$s orbital to the valence MO's to relax the antibonding interaction of the dσ and the CN^- σ orbitals, stabilizing a linear complex for Ag^+, Au^+, and Hg^{2+}.

Valence XPS. Figure 6 shows the valence XPS for linear cyanides as well as the calculated energy levels of the MO's with a significant metal d character. The lengths of the lines denote the extents of the metal d contribution, and are roughly proportional to the cross-section of photoionization, because the cross-sections of the d orbitals of heavy atoms are significantly larger than those of cyanide orbitals. For ready comparison, the position of the calculated energy-level of the δ_g orbital with esentially d character is arbitarily adjusted so as to coincide with the largest XPS peak of each spectrum. A reasonably good agreement is observed between the computed d level schemes and the experimental spectra. Thus the main peaks for the silver(I)

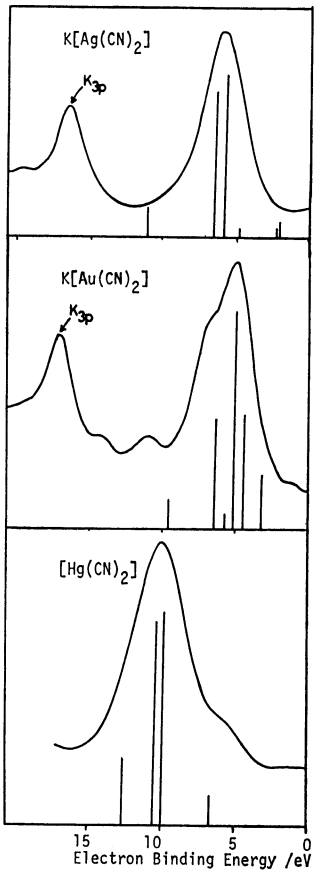

Fig. 6. Valence region of XPS and the orbital energy levels for $K[Ag(CN)_2]$, $K[Au(CN)_2]$, and $[Hg(CN)_2]$. Only the orbitals with large cross-sections are shown.

and gold(I) cyanide complexes appearing near 6.0 and 5.2 eV correspond to the $2\delta_g$ and $3\delta_g$ MO's, respectively. For the mercury(II) cyanide, the main peal at 10 eV is assigned to the $3\delta_g$ and $3\pi_g$ MO's overlapping each other. The complicated structure of the main peak for the Au^+ complex implies a strong interaction between Au and ligands.

Population Analysis. Table 3 gives the results of the Mulliken population analysis for linear dicyano complexes. The deviations of the effective metal charges (+0.42, +0.33, and +1.11) from formal charge for Ag^+, Au^+, and Hg^{2+} are respectively 0.58, 0.67, and 0.89, which show no remarkable difference in the net ligand-to-metal electron donation between uni- and bi-valent metals.

The net negative charge on carbon is largest in the Hg^{2+} complex. This might seem to be in conflict with the conventional argument that the ligand-to-metal electron donation would occur most extensively in the Hg^{2+} complex. However, the consideration of π back-donation will explain the puzzling situation. The variation of carbon charge among these complexes is mainly due to that in the Cpπ population (1.80 for Ag^+, 1.79 for Au^+, and 1.93 for Hg^{2+}). The change in nitrogen charge also results from that in the NPπ population (2.27, 2.27, and 2.07). Since the π back-donation causes a decrease in the carbon population and an increase in nitrogen population, the values of the

Table 3. The mulliken populations for linear dicyano complexes

		$[Ag(CN)_2]^-$	$[Au(CN)_2]^-$	$[Hg(CN)_2]$
Orbital populations (number of electrons)				
Metal	$d\sigma$	1.82	1.77	1.88
	$d\pi$	3.82	3.86	3.94
	$d\delta$	4.00	4.00	4.00
	s	0.71	0.83	0.79
	p	0.22	0.23	0.29
	Charge	+0.42	+0.33	+1.11
Carbon	2s	1.27	1.29	1.22
	$2p\sigma$	1.15	1.09	1.10
	$2p\pi$	1.80	1.79	1.93
	Charge	−0.22	−0.17	−0.26
Nitrogen	2s	1.71	1.72	1.72
	$2p\sigma$	1.52	1.50	1.51
	$2p\pi$	2.27	2.27	2.07
	Charge	−0.50	−0.49	−0.30
Bond overlap populations				
M–C	σ	0.36	0.40	0.41
	π	0.08	0.07	0.05
C–N	σ	0.38	0.41	0 41
	π	0.88	1.05	1.09

$Cp\pi$ and $Np\pi$ populations show that the π back-donation is smallest in the Hg^{2+} complex. On the other hand, the sum of the Cs and $Cp\sigma$ populations is smallest in the Hg^{2+} complex, indicating that the σ donation is largest in this complex. Both the smallest π back-donation and the largest σ donation is consistent with the highest electronegativity of Hg^{2+}.

The bond overlap populations of M–C and C–N increase in the orders of $Ag^+ < Hg^{2+} < Au^+$ and $Ag^+ < Au^+ < Hg^{2+}$, respectively. The infrared results show the orders of $Ag^+ < Hg^{2+} < Au^+$ and $Ag^+ < Au^+ < Hg^{2+}$ for the force constants of the M–C and C–N bonds,[14] respectively. The good agreement between the orders of the bond overlap populations and of the force constants may suggest that both of them are closely related to the bond strength.

The computations reported in this paper have been carried out on the HITAC M-180 computer of the Institute for Molecular Science.

References

1) L. E. Orgel, *J. Chem. Soc.*, **1958**, 4186.
2) W. R. Mason, *J. Am. Chem. Soc.*, **95**, 3573 (1973).
3) M. Sano, Y. Hatano, and H. Yamatera, *Chem. Phys. Lett.*, **60**, 257 (1979).
4) M. Sano, Y. Hatano, H. Kashiwagi, and H. Yamatera, *Bull. Chem. Soc. Jpn.*, **54**, 1523 (1981).
5) M. Sano, H. Adachi, and H. Yamatera, *Bull. Chem. Soc. Jpn.*, **54**, 2898 (1981).
6) M. Sano, H. Adachi, H. Kashiwagi, and H. Yamatera, The 29th Symposium on Coordination Chemistry of the Chemical Society of Japan, Hamamatsu, Oct. 1979.
7) H. Adachi, S. Shiokawa, M. Tsukada, C. Satoko, and S. Sugano, *J. Phys. Soc. Jpn.*, **47**, 1528 (1979).
8) For a review of the Hartree–Fock–Slater model, see J. C. Slater "Quantum Theory of Molecules and Solids," McGraw-Hill, New York (1974), Vol. 4.
9) E. J. Baerends and P. Ros, *Chem. Phys.*, **2**, 52 (1973).
10) H. Adachi, M. Tsukada, and C. Satoko, *J. Phys. Soc. Jpn.*, **45**, 875 (1978).
11) M. Sano, Y. Hatano, and H. Yanatera, *Chem. Lett.*, **1979**, 789.
12) S. Inagaki, H. Fujimoto, and K. Fukui, *J. Am. Chem. Soc.*, **98**, 4504 (1976).
13) The relative electron densities of the 4σ orbital on the C and N atoms are reversed by a slight mixing (10%) of the 5σ orbital; those of the 5σ orbital are also reversed by a slight orbital mixing.
14) L. H. Jones, *Inorg. Chem.*, **2**, 777 (1963).